

Attowatt Sensitivity of the Cold-Electron Bolometer

I. J. Agulo^{1(a)}, L. Kuzmin^{1(b)}, M. Tarasov¹

¹Chalmers University of Technology, Department of Microtechnology and Nanoscience, SE-412 96 Gothenburg, Sweden

^(a)On study leave at the University of the Philippines Baguio, Governor Pack Road, 2600 Baguio City, Philippines

^(b)Moscow State University, Nuclear Physics Institute, 119899 Moscow, Russia

We have fabricated and characterized the capacitively coupled Cold-Electron Bolometer (CEB) in the current-biased mode. We measured the bolometer responsivity and the noise equivalent power (NEP) by applying a modulated current through the heating tunnel junctions and absorber. The frequency of modulation varied from 35 Hz to 2 kHz. The best responsivity of 1.5×10^{10} V/W was obtained at 35 Hz. The NEP of better than 10^{-18} W/Hz^{1/2} was measured for frequencies above than 100 Hz. The background power load and the bolometer time constant were also estimated using the experimental device parameters.

The latest discoveries [1,2] in the field of astronomy have sparked increased interests in the field of space detector technology. These discoveries include the precise estimation of the age, composition and the geometry of the universe, and firmly established the big bang theory. In addition, measurements of the spectrum of the cosmic microwave background radiation supports the theory of an accelerating universe. However, the theory does not say what this dark energy (the “force” pushes the universe to expand) is. The pursuit to understand the nature of the dark energy and dark matter is what drives astronomers and physicists today. To accomplish this mission, a new generation of bolometers with increased sensitivity is required. The highest level of requirements for detectors in the near future will be determined by the proposed NASA missions SPIRIT, SPECS and SAFIR [3]. The detector goal is to provide noise equivalent power down to 10^{-20} W/Hz^{1/2} over the 40 – 500 μ m wavelength range in a 100x100 pixel detector array with low power dissipation array readout electronics. Inspired by these successes and motivated by the common goal of the knowledge about the origin of the universe, a new detector concept, called the Cold-Electron Bolometer (CEB) has been proposed [4,5].

The CEB concept is based on the direct electron cooling of the absorber that serves as a strong electrothermal feedback for the incoming signal. The electromagnetic signal is received and concentrated by a large antenna and through the capacitance of the superconductor-insulator-normal metal (SIN) tunnel junction is supplied and converted into heat in the the absorber with a small volume. The increase in energy of the electron in the absorber is equal to the energy of a photon. After the electron relaxes its energy, there are two ways where this energy will go. The electrons can transfer its energy to the normal metal phonons, which is a relatively slow process. The much faster process is the cooling of the electrons by the SIN tunnel junctions, by removing heat to the superconducting electrodes. The noise properties and sensitivity of the device are considerably improved by

decreasing the electron temperature in the absorber.

Electron cooling of the absorber improves the detector responsivity and sensitivity. The electron temperature, T_e , is coupled to the incoming power which we want to measure. In the HEB concept, T_e is always greater than the phonon temperature, T_{ph} . In the CEB concept, T_e is kept well below T_{ph} due to the strong electrothermal feedback. The feedback

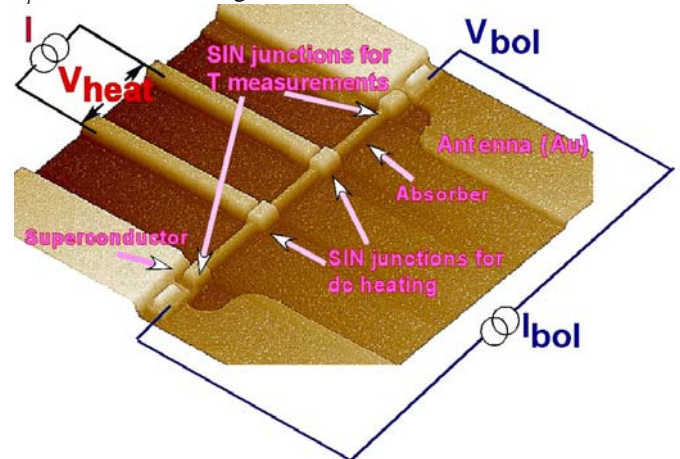


Fig. 1. (color online) Atomic force microscope image of a typical sample. It is composed of 4 superconductor-insulator-normal metal tunnel junctions and the normal metal absorber. The two outer SIN junctions can act as electron coolers of the absorber. Electron cooling is enhanced considerably by the gold trap, situated 0.5 μ m from the junctions. The inner tunnel junctions were used to measure the electron temperature of the absorber. In measurements of bolometer response, the inner junctions were used to apply heat to the absorber. The total volume of the absorber was 0.11 μ m³.

also increases the dynamic range of the device.

The non-equilibrium theory of the hot-electron bolometer (HEB) has been explained in detail by Golubev and Kuzmin [6]. As described previously, the T_e in the CEB is kept well below T_{ph} . This is achieved by improving the geometry of the superconducting electrodes such that there is more space for tunneled quasiparticles to diffuse into. The electron cooling can be further enhanced by adding normal metal traps adjacent to the superconducting electrodes. In our previous work [7,8], we demonstrated a decrease in electron temperature by almost 200 mK with the use of the normal

TABLE I
LIST OF EXPERIMENTAL PARAMETERS

	Area (μm^2)	Normal Resistance (k Ω)	Zero-bias Resistance (M Ω)
Outer SIN tunnel junctions	0.45	4.3	8.4
Inner SIN tunnel junctions	0.06	14.5	21.2
Normal metal absorber	0.11 μm^3 ^a	0.063	-

Measured parameters at 20 mK. The normal resistance corresponds to the asymptotic resistance for large bias currents.

^aThe volume of the absorber is the important parameter as it is directly coupled to the absorbed power and therefore to the sensitivity of the device.

metal traps. The only effect of this is to increase the cooling power of the SIN tunnel junction. This cooling power is described in equation (2) below.

As previously stated, the electron temperature of the absorber is directly related to the power of the incoming radiation, which we are interested in measuring. In order to determine the electron temperature of the normal metal absorber, one has to take into account all the contributions to the heat load to the absorber. The total power contribution at a given bias voltage at a certain temperature will determine the electron temperature. This can be attained by solving the heat balance equation, as shown below:

$$c_v \nu \frac{dT}{dt} + \Sigma \nu (T_e^5 - T_{ph}^5) + P(V, T_e, T_S) = P_0 + 2 \frac{V^2}{R_S} + \delta P(t) \quad (1)$$

where $c_v = \gamma T_e$ is the specific heat of the normal metal, ν is its volume, $\Sigma \nu (T_e^5 - T_{ph}^5)$ is the heat flow from the electron to the phonon sub-system in the normal metal, Σ is the electron-phonon coupling constant dependent on the material used, ν is the volume of the absorber, $2V^2/R_S$ [8,9] is the heat load due to the subgap leakage resistance, R_S , P_0 is the background power load of the bolometer, $\delta P(t)$ is the incoming rf power. The cooling power, $P(V, T_e, T_S)$, of the SIN tunnel junction is given by:

$$P(V, T_e, T_S) = \int dE E [\Gamma_{N \rightarrow S}(E) - \Gamma_{S \rightarrow N}(E)] \quad (2)$$

In the calculations, the temperature of the superconductor, T_S is assumed to be equal to the phonon temperature, T_{ph} . This assumption is valid only when the heating of the superconducting electrodes does not significantly affect the cooling power of the tunnel junctions, as in the case of the CEB.

A bolometer is characterized by its responsivity, sensitivity and the time constant. In the current-biased mode, the responsivity, S_V , is described by the voltage response to an incoming power

$$S_V(\omega, I) = \frac{\delta V_\omega}{\delta P_\omega} = \frac{-\frac{\partial I / \partial T}{\partial I / \partial V}}{-i\omega c_V \nu + 5\Sigma \nu T_e^4 + \frac{\partial P}{\partial T} - \frac{\partial I / \partial T}{\partial I / \partial V} \frac{\partial P}{\partial V}} \quad (3)$$

The noise is characterized by the Noise Equivalent Power (NEP), which is the net effect of all the sources referred to the

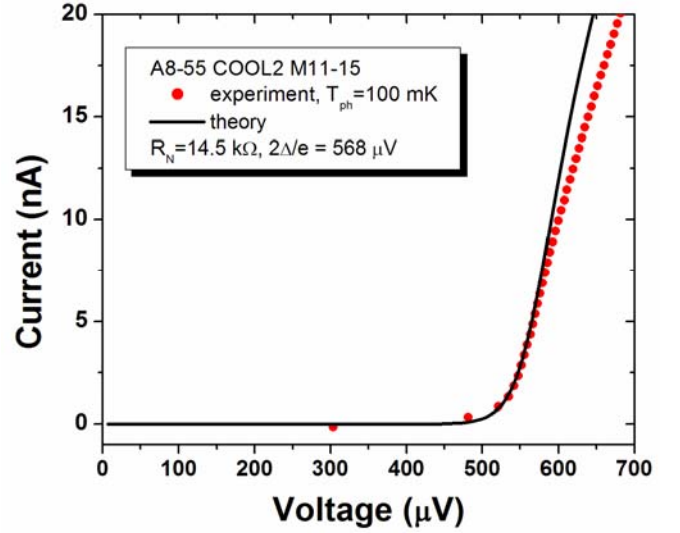


Fig. 2. (color online) Current-voltage characteristic of the tunnel junctions used for response measurements (the inner pair) at $T_{ph}=100$ mK (circles). The measured normal state resistance was 14.5 k Ω and the subgap resistance was 21.2 M Ω . The superconducting gap, $2\Delta=570$ μeV , was estimated by fitting the theoretical curve (solid line) with the experimental curve.

input of the bolometer. The total NEP is the sum of three components given by

$$\text{NEP}_{\text{total}}^2 = \frac{\langle \delta V_\omega^2 \rangle_{\text{amp}}}{S_V^2(0, I)} + 10k_B \Sigma V (T_e^6 + T_{ph}^6) + \text{NEP}_{\text{SIN}}^2 \quad (4)$$

The first term is the NEP due to the amplifier given by the voltage noise of the amplifier divided by the voltage response of the bolometer to applied power. The second term is the NEP associated with the heat flow between electrons and phonons. The last term is the NEP associated with SIN tunnel junction. Theory predicts that the CEB should be able to show a sensitivity of 10^{-19} W/Hz^{1/2} [4,6]. This paper demonstrates a sensitivity of better than 10^{-18} W/Hz^{1/2} at 100 mK in the current-bias mode.

The CEB is fabricated by e-beam lithography using two-layer resist technology, and two-angle evaporation. 0.2 μm PMMA on top of 0.8 μm Copolymer were exposed to 80 pA of beam current with a dose of 315 $\mu\text{C}/\text{cm}^2$. PMMA was developed in Toluene:IPA=1:3 and Copolymer in Ethoxylacetate:Ethanol=1:5 to create the e-beam masks for the device pattern. The normal metal traps and the bolometer device were made in two separate vacuum cycles. In the first vacuum cycle, 10 nm of chromium, followed by 30 nm of gold, and finally 10 nm of palladium were thermally evaporated to make 50 nm of normal metal trap. Cr was used for better adhesion of Au to the SiO₂ substrate. Pd was used as a buffer layer between Au and Al when they are in contact with each other. In time, Au reacts with Al forming an alloy that increase the contact resistance, which is naturally undesirable.

In the second vacuum cycle, the aluminum electrode was thermally evaporated at an angle of 55° relative to the surface normal up to a thickness of about 60 nm. The tunnel barrier

was formed by oxidizing the electrode for 2 minutes at a pressure of 5×10^{-2} mbar. The normal metal absorber was created by evaporating 30 nm of chromium and then 30 nm of copper at an angle of 0° . Cr was used to improve the impedance matching of the antennae to the normal metal and also for better adhesion of Cu to the substrate. Finally, the e-beam resist was removed by lift-off in acetone. Table 1 lists down the experimental parameters of the CEB.

The sample was measured in an Oxford dilution refrigerator. Measurements were performed in the current-biased mode. The current source consisted of a symmetric voltage source in series with bias resistors ranging from 200 k Ω to 20 G Ω . This provides us the possibility to measure large voltage ranges to measure the asymptotic resistances of the junctions, in addition to the subgap and zero-bias resistances. The high-ohmic bias resistances also provide some degree of protection from external interference.

Figure 1 shows a schematic of the CEB. It is composed of four SIN tunnel junctions and a normal metal absorber strip. The gold traps are adjacent to the two outer tunnel junctions. The input power is applied to these tunnel junctions, which heats up the absorber. The change in temperature of the electrons in the absorber is seen as a response in the voltage across the two inner tunnel junctions, which is then read out by an amplifier. We have also measured in the reverse configuration, where heating is applied through the inner tunnel junctions and the response is read from the outer tunnel junctions. The background power load into the absorber was estimated by measuring the dependence of voltage on phonon temperature for different bias currents and then compared our data to the theory. The optimal bias current was 20 pA, and the background power load was estimated to be 22 fW. The electron temperature of the absorber was determined by fitting the dependence of the voltage across the inner junctions at an optimal bias current to temperature with the theory. The superconducting gap voltage was 570 μ eV, obtained from fitting the I-V curve of the inner tunnel junctions with the theory (fig. 2).

The voltage responsivity, S_V , was measured by applying a heating current at different frequencies through the outer SIN tunnel junctions and measuring the voltage response across the inner tunnel junctions with the SR830 lock-in amplifier (see inset in fig. 3b for basic schematic of the measurement set-up). The signal generated by the internal oscillator of the SR830 lock-in amplifier was biased with a resistor to produce the heating current. The dependence of the response was then measured as a function of the bias current through the inner junctions. Using the current-voltage characteristics of the inner junctions, the bias current was converted to bias voltage. The response was then divided by the heating power, obtained from the current-voltage characteristics of the outer junctions. The typical result is the dependence of the responsivity for heating power of 0.2 fW on the bias voltage at 120 Hz, shown in figure 3a. For comparison the responsivity obtained with DC heating and the theoretical calculation was also plotted. The frequency dependence of the maximum was measured response from 35 Hz to 2 kHz and is shown in figure 3b. The

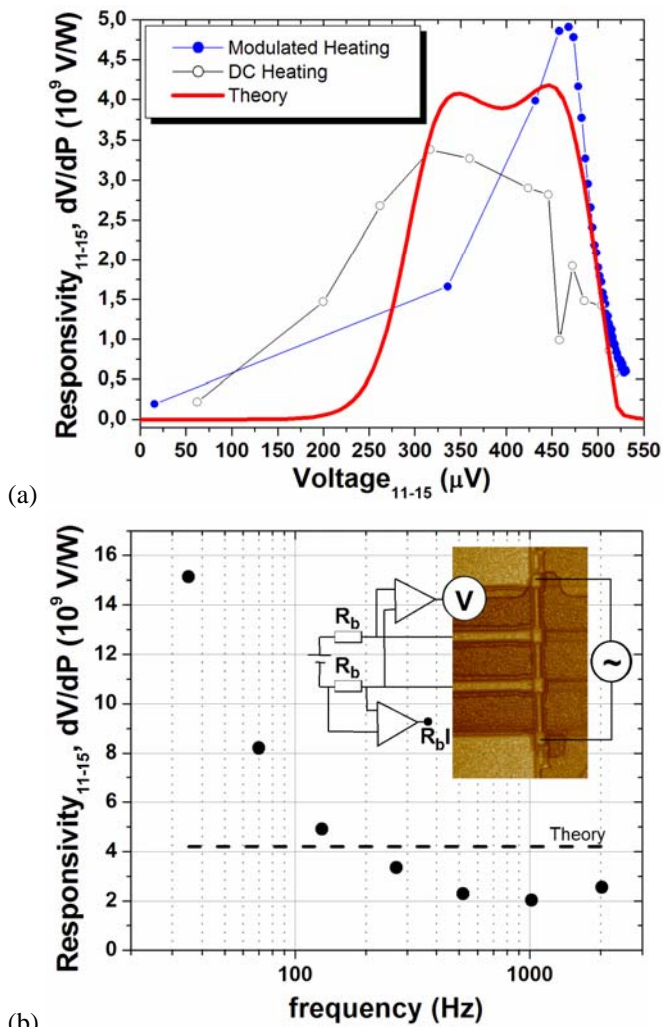


Fig. 3. (color online) (a) The responsivity of the cold-electron bolometer for heating power of 0.2 fW for a frequency of 120 Hz (solid circles) in comparison to responsivity due to DC heating (open circle) and theory (line). (b) The dependence of the responsivity on the frequency of modulation of the heating current. The dashed line represents the value of the maximum responsivity predicted by theory. (inset) The schematic for measuring responsivity of the CEB.

maximum value of the responsivity obtained was 1.5×10^{10} V/W measured at 35 Hz. The maximum value of the theoretical responsivity was 4.2×10^9 V/W and is shown as the dashed line in figure 3b.

The bolometer NEP was estimated. The bolometer NEP is obtained by first measuring the total NEP from the measured voltage noise at the output of the preamplifier divided by the measured responsivity of the device. It is then obtained by subtracting the contribution of the NEP of the amplifier from the total NEP . Figure 4a shows the bolometer, total and amplifier NEP s measured at 1 kHz in comparison to the theory. The frequency dependence of the total NEP , bolometer NEP and NEP of the amplifier from 35 Hz to 2 kHz is shown in figure 4b. The dashed lines show the theoretical calculations of the bolometer, total and amplifier NEP . As seen in the figure, the bolometer NEP is better than 10^{-18} W/Hz $^{1/2}$ for frequencies above 100 Hz. Theory predicts that the bolometer NEP was 0.5×10^{-18} W/Hz $^{1/2}$.

Finally, the time constant of the device is estimated from theory for the measured tunnel junction and absorber parameters. The time constant is given by $\tau = \gamma T_e V / (\partial P_{total} / \partial T)$, where $\gamma = 9.77 \text{ J}/\mu\text{m}^3\text{K}^2$ for copper. In the region below the gap at the optimal bias point, the bolometer time constant is 6.3 μs .

The theory agrees quite well with the I-V characteristics in the region below gap. We believe that a possible reason for the discrepancy between theory and experiment in the I-V curve in fig. 2 is due to the smearing of the superconducting gap.

For the responsivity measurements, good agreement between theory and experiment can also be seen in the region below and near the superconducting gap. The subgap resistance in the theory was modelled as V/R_S . The effect of this term can be seen in the absence of response below 200 μeV . A qualitative agreement in the region below and near the superconducting gap can also be seen between the theoretical prediction and the measured NEP (fig. 4a). The decreasing dependence of S_V and NEP in increasing frequency is attributed to the attenuation of the signal due to the cryogenic filters. The signal attenuation due to the read-out amplifiers was already factored in our analysis.

Our results illustrate that we are moving closer to the goal of an ultrasensitive microbolometer. The measured NEP better than $10^{-18} \text{ W/Hz}^{1/2}$, supported by the theoretical estimate of $0.5 \times 10^{-18} \text{ W/Hz}^{1/2}$ is the best ever achieved. The limitation is due to the voltage noise of the read-out amplifier. This can be improved by using an amplifier with lower voltage noise, or an amplifier in the cold stage to reduce its thermal noise and interference effects.

In future measurements, we intend to measure our bolometers in voltage-biased mode. Estimations made by Golubev and Kuzmin [6] yield better NEP in this mode. The reason for this is coincidence of the maximum responsivity and maximum electron cooling for voltage-biased mode. In the current-biased case, the maximum responsivity is shifted to lower voltages when maximum cooling is still near the superconducting gap. Another reason for measuring in the voltage-biased mode is that in this scheme the heat flow noise and the shot flow noise partially cancel each other, while in the current-biased mode, these two noise contributions are added together.

In summary, we have fabricated and characterized the cold-electron bolometer in the current-biased mode. The input power was a modulated heating current through the outer tunnel junctions and absorber with frequencies from 35 Hz to 2 kHz. The response was measured across the inner tunnel junctions. The best sensitivity obtained is better than $10^{-18} \text{ W/Hz}^{1/2}$ for modulation frequencies above 100 Hz.

We would like to thank Dmitry Golubev for extensive and enlightening discussions on the theoretical part of this work. This work was supported by The Swedish Research Council (Vetenskapsrådet), The Swedish Foundation for International Cooperation in Research and Higher Education (STINT), and the Swedish Institute (SI).

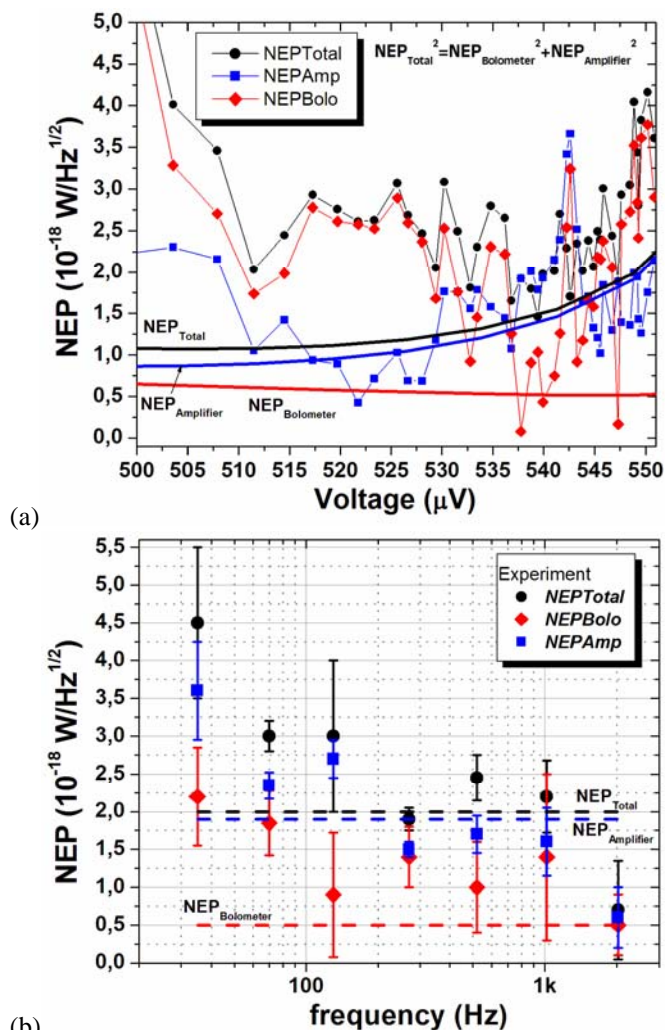


Fig. 4. (color online) (a) The measured total (circles), bolometer (diamonds) and amplifier (squares) NEP in comparison to theory. For these set of curves, the modulation frequency was 1.02 kHz. (b) The dependence of the total, bolometer and amplifier NEP to the modulation frequency. The dashed line represents the value of the NEPs as predicted by the theory.

REFERENCES

- [1] C. Seife, BREAKTHROUGH OF THE YEAR 2003: "Illuminating the Dark Universe," *Science*, vol. 302, iss. 5653, pp. 2038-2039, Dec. 2003.
- [2] W. Hu and M. White, "The Cosmic Symphony," *Scientific American*, pp. 45-53, Feb. 2004.
- [3] D. Leisawitz et al., "Scientific motivation and technology requirements for the SPIRIT and SPECS far-infrared/submillimeter space interferometers", *SPIE 2000*.
- [4] L. Kuzmin, "Ultimate cold-electron bolometer with strong electrothermal feedback," *Proceedings of SPIE -- Millimeter and Submillimeter Detectors for Astronomy II*, vol. 5498, pp. 349-361, Oct. 2004.
- [5] L. Kuzmin, "On the concept of a hot-electron microbolometer with capacitive-coupling of the antennae," *Proceeding of the 9th International Symposium on Space Terahertz Technology*, Pasadena, pp. 99-103, Mar. 1998; *Physica B: Condensed Matter*, vol. 284-288, pp. 2129-2130, part 2, Jul. 2000.
- [6] D. Golubev and L. Kuzmin, "Non-equilibrium theory of a hot-electron bolometer with normal metal-insulator-superconductor tunnel junction," *J. of Appl. Phys.*, vol. 89, no. 11, pp. 6464-6472, Jun. 2001.
- [7] I. J. Agulo, L. Kuzmin, M. Fominsky, and M. Tarasov, "Effective electron microrefrigeration by superconductor-insulator-normal metal

- tunnel junctions with advanced geometry of electrodes and with normal metal traps," *Nanotechnology*, vol. 15, no. 4, pp. S224-S228, Apr. 2004.
- [8] L. Kuzmin, I. J. Agulo, M. Fominsky, A. Savin, and M. Tarasov, "Optimization of electron cooling by SIN tunnel junctions," *Supercond. Sci. Technol.*, vol. 17, pp. S400-S405, May 2004.
- [9] A. Savin, M. Prunnila, J. Ahopelto, P. Kivinen, P. Törmä, J. Pekola, "Application of superconductor-semiconductor Schottky barrier for electron cooling," *Physica B*, vol. 329-333, pp. 1481-1484, May 2003.
- [10] L. Kuzmin, "Superconducting cold-electron bolometers with proximity traps," *Micr. Eng.*, vol. 69, pp. 309-316, 2003.